Atmospheric Research xxx (2012) xxx–xxx

Contents lists available at SciVerse ScienceDirect

Atmospheric Research

journal homepage: www.elsevier.com/locate/atmos

Gridded lightning climatology from TRMM-LIS and OTD: Dataset description

Daniel J. Cecil [a,*], Dennis E. Buechler [a], Richard J. Blakeslee [b]

[a] University of Alabama—Huntsville, 320 Sparkman Dr NW, Huntsville, AL 35808, USA
[b] NASA Marshall Space Flight Center, 320 Sparkman Dr NW, Huntsville, AL 35812, USA

ARTICLE INFO

Article history:
Received 28 February 2012
Received in revised form 11 May 2012
Accepted 14 June 2012
Available online xxxx

Keywords:
Lightning
Thunderstorm
Atmospheric electricity
TRMM

ABSTRACT

Gridded climatologies of total lightning flash rates observed by the spaceborne Optical Transient Detector (OTD) and Lightning Imaging Sensor (LIS) instruments have been updated. OTD collected data from May 1995 to March 2000. LIS data (equatorward of about 38°) adds the years 1998–2010. Flash counts from each instrument are scaled by the best available estimates of detection efficiency. The long LIS record makes the merged climatology most robust in the tropics and subtropics, while the high latitude data is entirely from OTD. The gridded climatologies include annual mean flash rate on a 0.5° grid, mean diurnal cycle of flash rate on a 2.5° grid with 24 hour resolution, mean annual cycle of flash rate on a 0.5° or 2.5° grid with daily, monthly, or seasonal resolution, mean annual cycle of the diurnal cycle on a 2.5° grid with two hour resolution for each day, and time series of flash rate over the sixteen year record with roughly three-month smoothing. For some of these (e.g., annual cycle of the diurnal cycle), more smoothing is necessary for results to be robust.

The mean global flash rate from the merged climatology is 46 flashes s^{-1}. This varies from around 35 flashes s^{-1} in February (austral summer) to 60 flashes s^{-1} in August (boreal summer). The peak annual flash rate at 0.5° scale is 160 fl km^{-2} yr^{-1} in eastern Congo. The peak monthly average flash rate at 2.5° scale is 18 fl $km^{-2}mo^{-1}$ from early April to early May in the Brahmaputra Valley of far eastern India. Lightning decreases in this region during the monsoon season, but increases further north and west. An August peak in northern Pakistan also exceeds any monthly averages from Africa, despite central Africa having the greatest yearly average.

1. Introduction

The spaceborne optical sensors Optical Transient Detector (OTD) on the MicroLab-1 satellite (later renamed OV-1) and Lightning Imaging Sensor (LIS) on the Tropical Rainfall Measuring Mission (TRMM) satellite have detected lightning for over sixteen years (1995–present) total. Christian et al. (2003) summarized the global lightning climatology based on OTD's five years of data (May 1995–March 2000). The lightning team associated with NASA Marshall Space Flight Center (MSFC) extended this to include a LIS-based gridded climatology and a merged LIS–OTD gridded climatology through 2005 (available from http://thunder.nsstc.nasa.gov). The LIS and LIS–OTD gridded climatologies are here extended with LIS data from Jan. 1998 to Dec. 2010. Results are similar to those found from the earlier climatologies, although the length of the current data record allows more detailed analyses with less spatial or temporal smoothing. The lightning climatology is drastically different from a rainfall climatology, for example from the TRMM-based rainfall climatologies presented by Adler et al. (2009).

The purposes of this paper are to announce the public availability of the gridded LIS–OTD climatology datasets, to describe those datasets, and to present analyses of these datasets. The gridded fields are listed in Table 1 and described in Section 2. Our intention is to update these annually, with the addition of LIS data for each subsequent year of TRMM.

* Corresponding author at: Earth System Science Center, University of Alabama—Huntsville, 320 Sparkman Dr NW, Huntsville, AL 35805, USA. Tel.: +1 256 961 7549.
E-mail address: cecild@uah.edu (D.J. Cecil).

0169-8095/$ – see front matter © 2012 Elsevier B.V. All rights reserved.
doi:10.1016/j.atmosres.2012.06.028

Table 1
Products in LIS–OTD gridded climatology files.

File identifier	Product name	Product description	Units	Product dimensions	Bin sizes	Smoothing
HRFC	HRFC_COM_FR HRFC_OTD_FR HRFC_LIS_FR	Mean annual flash rate	Flashes km^{-2} yr^{-1}	720×360	0.5°×0.5°	none
HRFC	HRFC_OTD_RF HRFC_LIS_RF	Raw flash count	Flashes	720×360	0.5°×0.5°	none
HRFC	HRFC_OTD_SF HRFC_LIS_SF	Flash count scaled by detection efficiency	Flashes	720×360	0.5°×0.5°	none
HRFC	HRFC_OTD_VT HRFC_LIS_VT	Viewtime (observation duration)	s km^2	720×360	0.5°×0.5°	none
LRFC	Same products as HRFC	Low-resolution version of HRFC	Flashes km^{-2} yr^{-1}	144×72	2.5°×2.5°	none
LRDC	Same products as HRFC	Mean diurnal cycle, in local solar time	Flashes $km^{-2}h^{-1}$	24×144×72	1 h×2.5°×2.5°	none
HRAC	HRAC_COM_FR HRAC_OTD_FR HRAC_LIS_FR	Annual cycle of flash rate	Flashes km^{-2} day^{-1}	365×720×360	1 day×0.5°×0.5°	2.5°×2.5° boxcar moving average, 111-day boxcar moving average, 110-day digital filter
LRAC	Same products as HRFC	Low spatial resolution annual cycle	Flashes km^{-2} day^{-1}	365×144×72	1 day×2.5°×2.5°	none
HRMC	HRMC_COM_FR HRMC_OTD_FR HRMC_LIS_FR	Mean flash rate in middle of each month, with monthly smoothing	Flashes km^{-2} day^{-1}	12×720×360	1 month×0.5°×0.5°	2.5°×2.5° boxcar moving average, 31-day boxcar moving average, 30-day digital filter
HRMC	HRSC_COM_FR HRSC_OTD_FR HRSC_LIS_FR	Mean flash rate in middle of each month, with seasonal smoothing	Flashes km^{-2} day^{-1}	12×720×360	1 month×0.5°×0.5°	2.5°×2.5° boxcar moving average, 91-day boxcar moving average, 91-day digital filter
LRADC	LRADC_COM_SMFR	Annual cycle of diurnal cycle (UTC) of flash rate	Flashes km^{-2} day^{-1}	365×6×144×72	1 day×4 h (UTC)×2.5°×2.5°	7.5°×7.5° boxcar moving average, 111-day boxcar moving average
LRADC	LRADC_COM_SMFR2	Annual cycle of diurnal cycle (UTC) of flash rate	Flashes km^{-2} day^{-1}	365×12×144×72	1 day×2 h (UTC)×2.5°×2.5°	As in SMFR, but with 55-day boxcar moving average
LRADC	LRADC_COM_SF	Flash count scaled by detection efficiency	Flashes	365×12×144×72	1 day×2 h (UTC)×2.5°×2.5°	
LRADC	LRADC_COM_VT	Viewtime (observation duration)	days km^2	365×12×144×72	1 day×2 h (UTC)×2.5°×2.5°	
LRTS	LRTS_COM_FR LRTS_COM_VT	Daily time series of flash rate and viewtime, 28 June 1995–25 Feb 2011	Flashes km^{-2} day^{-1}; days km^2	5716×144×72	1 day×2.5°×2.5°	7.5°×7.5° boxcar moving average, 111-day boxcar moving average, 110-day digital filter
LRTS	LRTS_OTD_FR LRTS_OTD_VT	Daily time series of flash rate and viewtime, 28 June 1995–28 January 2000	Flashes km^{-2} day^{-1}; days km^2	1676×144×72	1 day×2.5°×2.5°	7.5°×7.5° boxcar moving average, 111-day boxcar moving average, 110-day digital filter
LRTS	LRTS_LIS_FR LRTS_LIS_VT	Daily time series of flash rate and viewtime, 25 February 1998–25 February 2011	Flashes km^{-2} day^{-1}; days km^2	4749×144×72	1 day×2.5°×2.5°	7.5°×7.5° boxcar moving average, 99-day boxcar moving average, 98-day digital filter
LRMTS	LRMTS_COM_FR	Monthly time series of flash rate (weighted more toward LIS than other products)	Flashes km^{-2} day^{-1}	204×144×72	1 month×2.5°×2.5°	Weighted average of LRTS_OTD_FR and LRTS_LIS_FR
LRACTS	Same products as LRTS	Mean daily flash rate from time series product	Flashes km^{-2} day^{-1}	366×144×72	1 day×2.5°×2.5°	Same as LRTS

Please cite this article as: Cecil, D.J., et al., Gridded lightning climatology from TRMM-LIS and OTD: Dataset description, Atmos. Res. (2012), doi:10.1016/j.atmosres.2012.06.028

Projections suggest that the TRMM satellite may remain in orbit until 2015. Section 3 shows some examples of what can be found in these gridded fields, and how to choose between the related products. Some of these products are created at finer resolution than is justified by the sample sizes, and we leave it to the user to choose an appropriate way to handle the data for a given science application.

2. Data and methods

Details on the lightning sensors are provided by Christian et al. (2003) and Boccippio et al. (2002). Both sensors monitor the 777.4 nm atomic oxygen multiplet, detecting pulses of illumination (produced by lightning) above background levels. Both are (were) onboard satellites in low earth orbit, viewing an earth location for about 3 min as OTD passed overhead or 1.5 min as LIS passed overhead. Data files from each individual orbit are available from the Global Hydrology Resource Center (GHRC), with 14 orbits/day for OTD and 16 orbits/day for LIS. Lightning flash times and locations are recorded with approximately 10 km resolution from OTD and 5 km resolution from LIS. For a $0.5^\circ \times 0.5^\circ$ latitude–longitude grid, the orbit files also record which grid boxes are within the field of view with the instrument collecting data properly (i.e., quality control flags indicate acceptable conditions) individually for each second of the orbit. Many other lightning attributes and instrument information are included in the orbital files (for example, flash duration, radiance, and areal extent of the illumination).

For each grid box, the total viewtime (observation duration) and flash count are summed over all orbits, and sorted by time of day and day of year. Flash counts are scaled by each instrument's detection efficiency (Boccippio et al. 2002 and Christian et al. 2003), which varies with time of day. For the OTD, detection efficiency also varies with geographic location. The optical sensors can more easily discriminate lightning from the background scene at night, with bright daytime cloud tops being more difficult. Following Boccippio et al. (2002), the LIS detection efficiency ranges from about 69% near local noon to 88% overnight (Table 2). Different sensitivity thresholds were used with the OTD during the course of its mission, with the detection efficiency adjusted accordingly. The OTD detection efficiency is reduced roughly in half over the South Atlantic Anomaly. The detection efficiency values as a function of sensitivity thresholds, geographic location, and time of day are available in the data files for the gridded climatology. The mean values outside the South Atlantic Anomaly region are listed in Table 2.

The TRMM satellite (described by Kummerow et al., 2000) orbits between 35° N and S, so the LIS sampling is maximized near those latitudes. LIS has observed equatorial regions for a little over 100 h total (through the year 2010), and a band between 30 and 38° N and S for 200–400 h (Fig. 1a). With a typical sampling duration of ~90 s at a time, this equates to approximately 4000 separate observations of any point on the equator, and 8000–16,000 observations of each location in the subtropics. Adding the five years of OTD yields a combined viewtime grid (Fig. 1b) with just over 150 h recorded at the equator, around 65 h immediately poleward of the edge of LIS's field of view (~38° N and S), and 240 h near 75° N and S. High noise rates within the South Atlantic Anomaly region reduce the effective OTD viewtime near Brazil, but LIS is only marginally affected due to its lower altitude orbit.

Table 2
Detection efficiencies applied to estimate flash rates and scaled flash counts in LIS–OTD gridded climatologies. OTD detection efficiency varies with location and with sensor threshold settings, as specified in the available data files; its mean value is listed in table.

Local hour	LIS	OTD
00–01	0.880000	0.486554
01–02	0.879994	0.495009
02–03	0.879999	0.501647
03–04	0.880003	0.507448
04–05	0.879996	0.506446
05–06	0.876248	0.511522
06–07	0.849902	0.518423
07–08	0.812438	0.501935
08–09	0.763066	0.471787
09–10	0.737929	0.425287
10–11	0.712149	0.389866
11–12	0.692533	0.377269
12–13	0.695175	0.377390
13–14	0.714210	0.396366
14–15	0.734270	0.431355
15–16	0.758117	0.476192
16–17	0.802531	0.510014
17–18	0.843822	0.518428
18–19	0.875470	0.510989
19–20	0.879903	0.504840
20–21	0.879999	0.505231
21–22	0.879999	0.497961
22–23	0.880001	0.491061
23–24	0.879995	0.485675

The TRMM satellite was boosted from an average altitude of about 350 km before August 2001 to about 400 km after August 2001. The higher altitude gives a correspondingly larger field of view for each sensor pixel, and for the swath. Since a lighting flash typically illuminates a cloud top area significantly larger than the field of view of a LIS pixel and since the LIS detection threshold settings were not changed after boost, one would not expect any change in detection efficiency because of the boost and this has been confirmed by analysis of the data. The higher orbit also gives a slightly longer sampling duration. This increases the total flash *counts*, but not the flash *rates*.

The gridded LIS–OTD climatology products are described below and summarized in Table 1. Although some products have different units, most figures and animations in this paper scale the flash rates to flashes km^{-2} yr^{-1}, in order to make easy comparisons with the same color scale. There are a few ways the products could be computed, whether accounting for sampling limitations differently, smoothing, changing the units, or merging the LIS and OTD data differently. Because many users have downloaded and used previous versions of this dataset, we choose to retain the same methodology, format, and smoothing as in those previous releases. GHRC has served 117 GB worth of previous versions of this dataset to around 250 registered users from 42 countries, besides 347 GB to an unknown number of users by anonymous ftp.

Please cite this article as: Cecil, D.J., et al., Gridded lightning climatology from TRMM-LIS and OTD: Dataset description, Atmos. Res. (2012), doi:10.1016/j.atmosres.2012.06.028

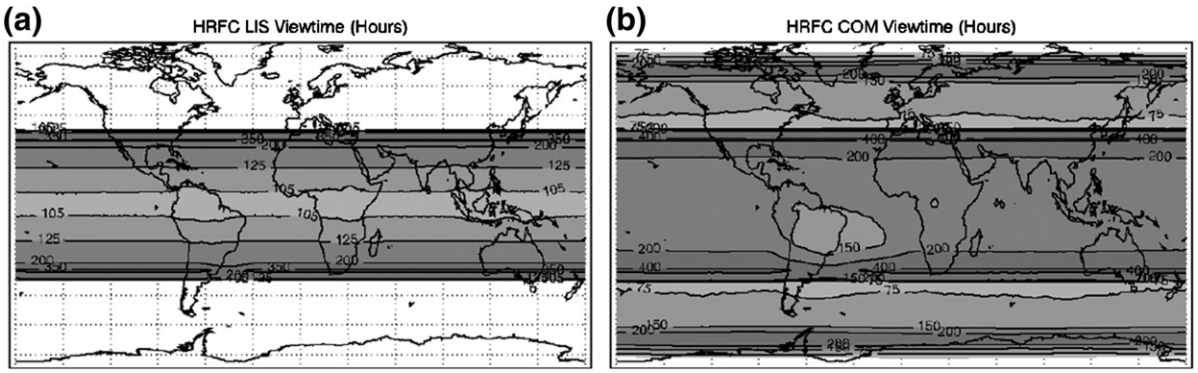

Fig. 1. Accumulated viewtime in hours for (a) LIS from 1998 to 2010 and (b) OTD plus LIS from 1995 to 2010. Viewtime from OTD alone is the same as shown in Fig. 1 of Christian et al. (2003).

2.1. High resolution flash climatology (HRFC) and low resolution flash climatology (LRFC)

From each orbit, the total number of detected flashes and the total viewtime are accumulated on both a high resolution (0.5°×0.5°) grid and a low resolution (2.5°×2.5°) grid. The raw flash count is accumulated (abbreviated RF), and a scaled flash count (SF) is computed using the appropriate detection efficiency. For example, if LIS detects a flash between 00 and 01 local solar time, it is counted as one raw flash and 1/0.88 = 1.14 scaled flashes (using the detection efficiency listed in Table 2). The viewtime (VT) is recorded with units s km^2, with the observation duration (s) multiplied by the size of the 0.5° grid box (km^2). The flash rate (FR) is computed as FR = 86,400 * 365.25 * (SF/VT), with units flashes yr^{-1} km^{-2}. These values are accumulated and stored separately for LIS and OTD. A combined flash rate is computed simply as COM_FR = 86,400 * 365.25 * (OTD_SF + LIS_SF)/(OTD_VT + LIS_VT). This is the simplest approach possible, and implicitly assumes that all locations are adequately sampled with regard to time of day, time of year, or any other source of bias. In all subsequent products described below, flash rate is also computed using scaled flashes, and the combined flash rate is computed using (OTD_SF + LIS_SF)/(OTD_VT + LIS_VT) unless otherwise noted.

In some places with low flash rates (mostly oceans and arid regions), or at high latitudes with limited sampling from OTD only, the high resolution flash climatology (HRFC) data appear a bit noisy (Fig. 2a) because the sampling is insufficient for such a high resolution. On the other hand, LRFC (Fig. 2b) appears smoother than necessary over land, especially in the tropics. We prefer to make the data available at both resolutions, so the user may apply whatever smoothing seems appropriate for a given application. In some tropical locations where high flash rates are linked to topographic features, an even finer resolution may be acceptable (Albrecht et al. 2011).

2.2. Low resolution diurnal climatology (LRDC) and low resolution annual climatology (LRAC)

The low resolution diurnal climatology (LRDC) is compiled the same way as LRFC, except that the flashes and viewtimes are assigned to 1 h (local solar time)×2.5°×2.5° bins when accumulating from each orbit. The flash rate for LRDC is stored in units of flashes h^{-1} km^{-2}. The amplitude of the diurnal cycle is much stronger over land than ocean, with a peak between 1500 and 1700 LST (Supplementary animation LRDC_COM_FR.mov—1.2 MB). The low resolution annual climatology (LRAC) assigns flashes and viewtimes to bins of one day×2.5°×2.5°. The LRAC flash rate is stored in units of flashes day^{-1} km^{-2}. As with HRFC, hourly binning in LRDC and daily binning in LRAC leave sample sizes that are too small to be robust, and we leave it to the user to choose an appropriate smoothing. Smoothing is especially needed for LRAC, which is obvious from an animation of the daily values (Supplementary animation LRAC_COM_FR.mov—15.5 MB).

2.3. High resolution annual climatology (HRAC)

The high resolution annual climatology (HRAC) assigns flashes and viewtimes to daily 0.5°×0.5° bins, but adds substantial smoothing. A 2.5°×2.5° boxcar moving average is applied to the 0.5° grid points. More importantly, a 111-day boxcar moving average is applied to the flash counts and viewtimes before computing flash rates. Then a low pass digital filter is applied to the flash rates. This makes HRAC suitable for a smooth animation of the annual cycle of lightning flash rate (Supplementary animation HRAC_COM_FR.mov—18 MB), but the precise daily value should not be taken too seriously after more than three months' worth of smoothing has been applied.

2.4. High resolution monthly climatology (HRMC) and high resolution seasonal climatology (HRSC)

The high resolution monthly climatology (HRMC) and high resolution seasonal climatology (HRSC) are similar to HRAC, except with less temporal smoothing and with only 12 entries per year instead of 365. They begin with the HRAC grids that have data binned as one day×0.5°×0.5°, before any smoothing is applied. A 2.5°×2.5° boxcar moving average is applied (as in HRAC), then a 31-day boxcar moving average and low pass digital filter are applied for HRMC (Supplementary animation HRMC_COM_FR.mov), and a 91-day boxcar moving average and low pass filter are applied

Please cite this article as: Cecil, D.J., et al., Gridded lightning climatology from TRMM-LIS and OTD: Dataset description, Atmos. Res. (2012), doi:10.1016/j.atmosres.2012.06.028

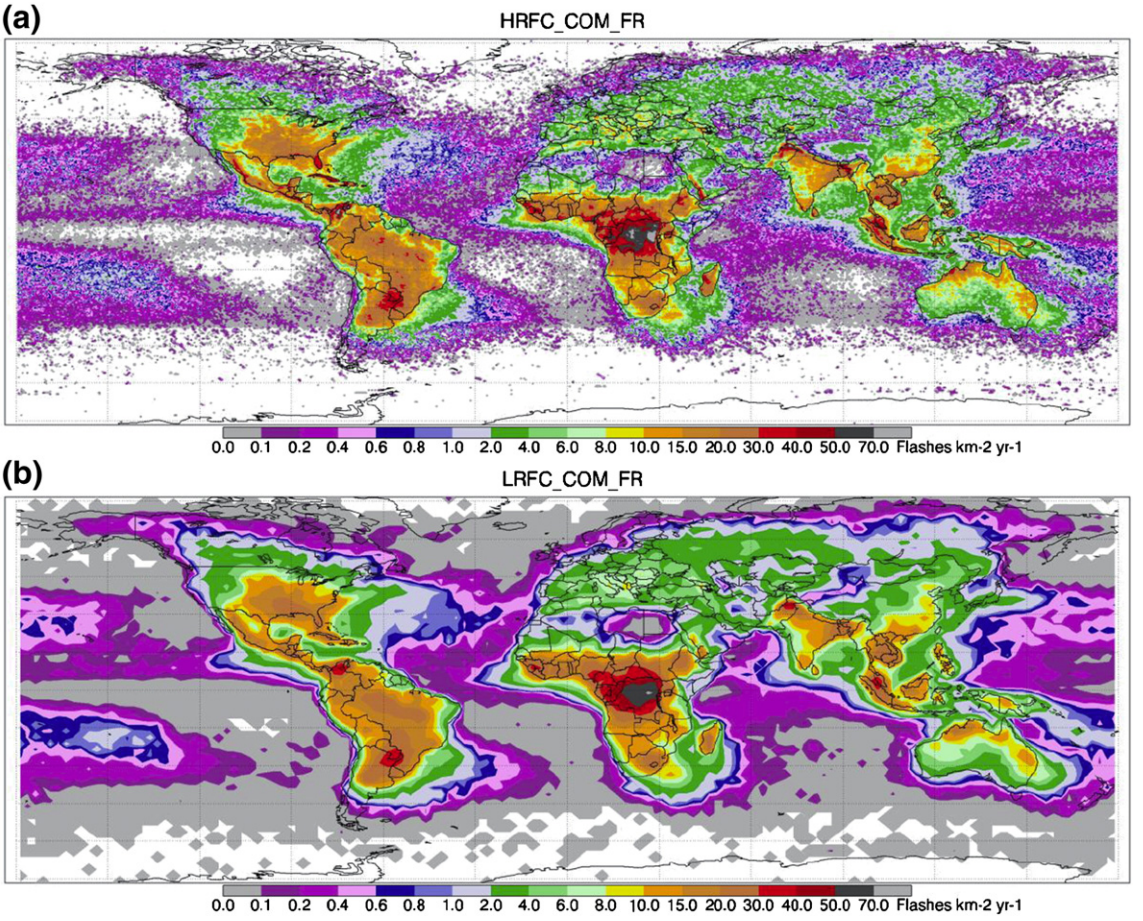

Fig. 2. (a) HRFC mean annual flash rate from combined LIS and OTD, 0.5° grid. (b) LRFC mean annual flash rate from combined LIS and OTD, 2.5° grid.

for HRSC (Supplementary animation HRSC_COM_FR.mov). After this smoothing, the daily average flash rate is extracted from the middle of each month. HRMC and HRSC thus store the daily average flash rates for January 16, February 15, March 16, etc., with either monthly (HRMC) or three-monthly (HRSC) smoothing applied. As in LRAC and HRAC, the units are flashes day^{-1} km^{-2}.

A straightforward usage of HRMC is to map the flash rates for a particular month, or to animate a set of such maps. As an example of another usage, HRMC (or similarly HRSC, HRAC, or LRAC) can be used to examine the annual cycle of zonal-mean or meridional-mean flash rates (Fig. 3). Fig. 3 was created by multiplying the mean flash rates for each month in HRMC by the corresponding grid box area, and accumulating all latitudes for a given 0.5° longitude bin. For longitudes with lightning dominated by North America (roughly between 120° and 80° W), the flash rates increase during boreal spring and peak in August, then decline rapidly. Slightly further east, there is a shift in the month of highest flash rates from August around 75° W (dominated by Colombia and eastern Cuba) to September–October slightly to the east. This corresponds to the shift of the local lightning maximum from northern Colombia to Lake Maracaibo in northern Venezuela. Bürgesser et al. (2012) also showed an October lightning peak over Lake Maracaibo, using World Wide Lightning Location Network (WWLLN) observations. The longitudes with the remainder of South America are dominated by an October (austral spring) peak in both central Brazil and northern Argentina. The longitudes of west Africa have a broad peak in boreal summer. Central Africa (15°–30° E) has high flash rates all year, but thunderstorms during austral spring and summer in southern Africa contribute to a strong peak from those longitudes. Flash rates between about 70°–95° E are dominated by Pakistan, India, and Bangladesh. The westward progression of thunderstorm activity from pre-monsoon to monsoon season can be seen here, with high flash rates near Bangladesh (90° E) in April–May shifting across India and Pakistan for boreal summer and early autumn. Cecil and Blankenship (2012) inferred a similar seasonal shift in the locations of severe hailstorms across the Indian subcontinent. Southeast Asia has a sharp increase in lightning in April, contributing to the peak around 100° E. Further east there is a boreal summer peak of lightning associated with eastern China and an austral summer peak of lightning associated with Australia.

2.5. Low resolution annual diurnal climatology (LRADC)

The low resolution annual diurnal climatology (LRADC) is compiled by assigning flashes and viewtimes into daily,

Please cite this article as: Cecil, D.J., et al., Gridded lightning climatology from TRMM-LIS and OTD: Dataset description, Atmos. Res. (2012), doi:10.1016/j.atmosres.2012.06.028

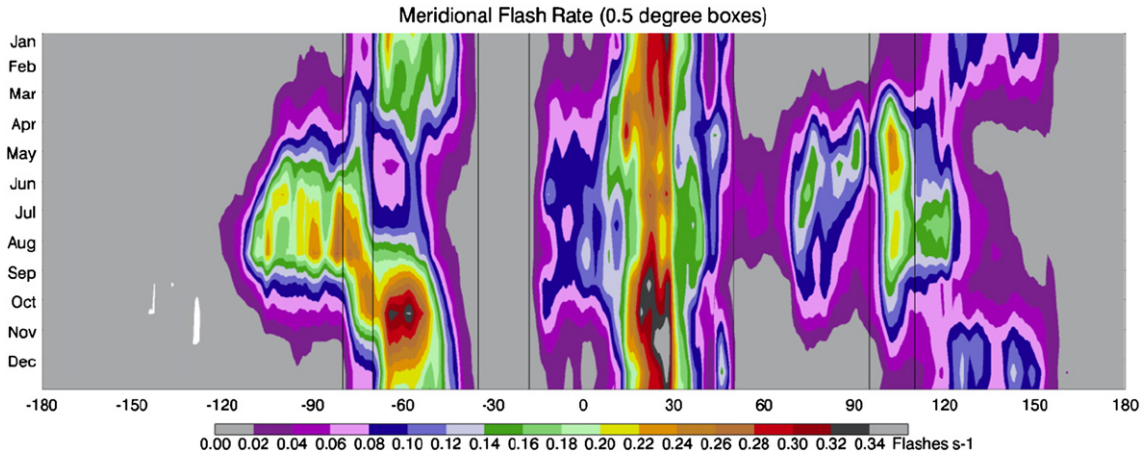

Fig. 3. Monthly progression of meridional-mean flash rates from HRMC, averaged along 0.5° bins of longitude. Units are flashes s^{-1} totaled over all latitudes for a particular longitude bin. Vertical lines roughly separate North America (west of 80° W), Colombia and Lake Maracaibo (between 80 and 70° W), much of the remainder of South America (between 70° and 35° W), Africa (between 18° W–50° E), and southeast Asia and Sumatra (between 95° and 110° E).

two-hourly bins on a 2.5°×2.5° spatial grid. Unlike in LRDC, the two-hourly bins are based on UTC time, not local time. So an animation of LRADC (Supplementary animation LRADC_COM_SMFR_small_slow.mov—29 MB) shows the highest flash rates progressing from east to west across the globe each day (as the local afternoon maximum progresses westward with the sun). The scaled flash count and viewtime grids are stored to the LRADC output file as 365×12×144×72 arrays, before any subsequent smoothing. To increase the sample sizes before computing flash rates, the flash counts and viewtimes are also assigned to daily, four-hourly (UTC) bins. The two-hourly and four-hourly grids are then smoothed with 7.5°×7.5° boxcar moving averages in space. A 111-day boxcar moving average is applied to the four-hourly grids, and a 55-day boxcar moving average is applied to the two-hourly grids. Thus the smoothed, four-hourly (UTC) flash rate (LRADC_COM_SMFR) has the most smoothing both in terms of hours per day and days per year. The two-hourly (UTC) flash rate (LRADC_COM_SMFR2) has more detail, at the expense of less robust sample sizes.

There is much room for confusion with the LRADC products, so a few things are pointed out here. The LRADC output file includes scaled flash count and viewtime *without* smoothing, so dividing the flash count by the viewtime from this file will *not* give the same answer as either of the smoothed flash rates included in the file. The LRADC smoothed flash rates have more spatial averaging than the products that were previously mentioned, so they will not give the same values at each grid point as either LRAC or LRDC. Finally, the LRADC viewtime array is stored with units of days km^2 instead of s km^2. These viewtime units differ from most of the other products, but maintain consistency with the previous release of this dataset, insuring compatibility with any prior user-developed software.

2.6. Low resolution time series (LRTS), low resolution annual climatology time series (LRACTS)

The low resolution time series (LRTS) gives a multi-year time series of the smoothed daily flash rate (Supplementary animation LRTS_COM_FR.mov—187 MB) and viewtime grid for each day of the satellite missions, minus an appropriate number of days at the beginning and end to allow for smoothing. For each day, the total number of scaled flashes and viewtime are compiled for the 2.5°×2.5° grid. A 99-day boxcar moving average is applied to the LIS scaled flash counts and viewtimes, while a 111-day boxcar moving average is applied to the OTD and combined scaled flash counts and viewtimes. These averaging periods are chosen to allow LIS and OTD to progress through the diurnal cycle at a given location twice. A 7.5°×7.5° boxcar moving average is then applied to the flash count and viewtime grids, they are divided to get the flash rate, and then a low pass digital filter is applied to both flash rate and viewtime. These smoothed flash rate and viewtime grids are stored with units of flashes day^{-1} km^{-2} and day km^2, respectively. Individual LRTS files store time series for LIS, OTD, and their combination, with the different periods of record specified in each file (and in Table 1).

Totaling all the lightning in the LRTS gives a multi-year estimate of the global flash rate (Fig. 4). OTD is unavailable after early 2000 and LIS only samples the tropics, so a correction to the LIS global flash rate is applied based on the ratio of OTD flashes between +/−35° to total global OTD flashes. This ratio is computed for each day of the year, and then applied to the LIS flash rate between +/−35°. Every year has a large oscillation between low flash rates in austral summer and high flash rates in boreal summer, because there is so much more land in the northern hemisphere than southern hemisphere. Inter-annual variability is obvious, but no significant trend is apparent. The minimum flash rate has varied from a little under 40 flashes s^{-1} during austral summer 2005–06 to a little over 30 flashes s^{-1} during austral summer 2006–07. The boreal summer peak flash rate has ranged from around 60 flashes s^{-1} in several years (1998, 1999, 2000, 2002, 2004, 2009) to around 55 flashes s^{-1} in others (1997, 2003, 2007, 2010).

The purpose of the low resolution annual climatology time series (LRACTS—Supplementary animation LRACTS_COM_FR.mov—11.8 MB) is to provide a baseline against which

Please cite this article as: Cecil, D.J., et al., Gridded lightning climatology from TRMM-LIS and OTD: Dataset description, Atmos. Res. (2012), doi:10.1016/j.atmosres.2012.06.028

LRTS can be compared for anomalies. For a given day of the year, that day is extracted from LRTS for each year and averaged. For example, 31 Oct has sixteen daily average flash rate grids in LRTS_COM_FR, for each year from 1995 to 2010. The LRACTS_COM_FR grid has the average flash rate from those sixteen years. The 31 Oct 1998 LRTS grid can be presented as an anomaly from the mean by subtracting the 31 Oct LRACTS_COM_FR grid. This could alternatively be done using the mean annual cycle in LRAC, except that there would be an inconsistency introduced by the lack of smoothing in LRAC.

2.7. Low resolution monthly time series (LRMTS)

The low resolution monthly time series (LRMTS) is similar to LRTS, but provides one grid per month instead of one per day (Supplementary animation LRMTS_COM_FR.mov). The merger of LIS and OTD data is handled differently with LRMTS than with any of the other products. The LRMTS output file only stores the combined flash rate, not the individual contributions from LIS and OTD. To produce LRMTS, LIS and OTD flash rates and viewtimes are smoothed precisely the same way as they were in LRTS. The flash rate and viewtime values are extracted for the middle day of each month. Then the combined flash rate for each grid box is computed as:

$$\begin{aligned}\text{LRMTS\_COM\_FR} = {} & (\text{OTD\_FR} * \text{OTD\_VT} * 0.47 \\ & + \text{LIS\_FR} * \text{LIS\_VT} * 0.87) \\ & / (\text{OTD\_VT} * 0.47 + \text{LIS\_VT} * 0.87).\end{aligned}$$

This weights the combination more toward LIS, because LIS has a greater detection efficiency (approximated here as 0.87) than OTD (0.47). LRMTS is the only product combining LIS and OTD this way. All other products treat the combination as in Section 2.1. Although potentially confusing, this maintains consistency with previous releases of this dataset. For years when only one sensor is available (OTD before 1998; LIS after 2000) or latitudes only sampled by OTD (poleward of 42.5°, after accounting for smoothing), the different approaches used for merger do not matter.

2.8. Future updates

Our intention is to update this dataset once per year through the remainder of the TRMM mission, and release data through the GHRC via http://thunder.nsstc.nasa.gov. The earliest LIS data we use is from 1 Jan 1998, so the LIS time series in LRTS begins in late February 1998 (to allow a full smoothing window). Extending this through late February of the current and subsequent years requires data into April for use in the smoothing. The end of the time series is more reliable if data from May are also used, because the low pass digital filter can give unrealistic results near the beginning and end. Therefore updates are expected to be released during boreal summer each year.

3. Comparing and choosing between related products

3.1. Mapping the total annual flash rate

Some science topics could be addressed using more than one of these products, with different results (or different requirements) depending on which is chosen. The mean annual flash rate grids HRFC and LRFC (Fig. 2) are the simplest and most popular (i.e., most downloaded by users) of these products. They portray the mean annual flash rate as a simple counting experiment, dividing the total number of flashes by the total observation duration. This assumes that the observations have been adequately distributed through the annual cycle and diurnal cycle at all locations. Alternatively, a mean flash rate at each latitude–longitude grid point in HRAC or LRAC would ensure that each day of the year is weighted equally. A mean flash rate from LRDC would ensure that each hour of the day is weighted equally. A mean flash rate from LRADC accounts for both the day of year and time of day.

In the tropics and subtropics where sampling is good due to the long record of LIS observations, the mean annual flash rate from LRADC agrees to within 10% with that from LRFC (Fig. 5). In many places, the agreement is within 1%. At higher latitudes where only OTD was available and the sampling is poor (Fig. 1), the agreement between these estimates (and

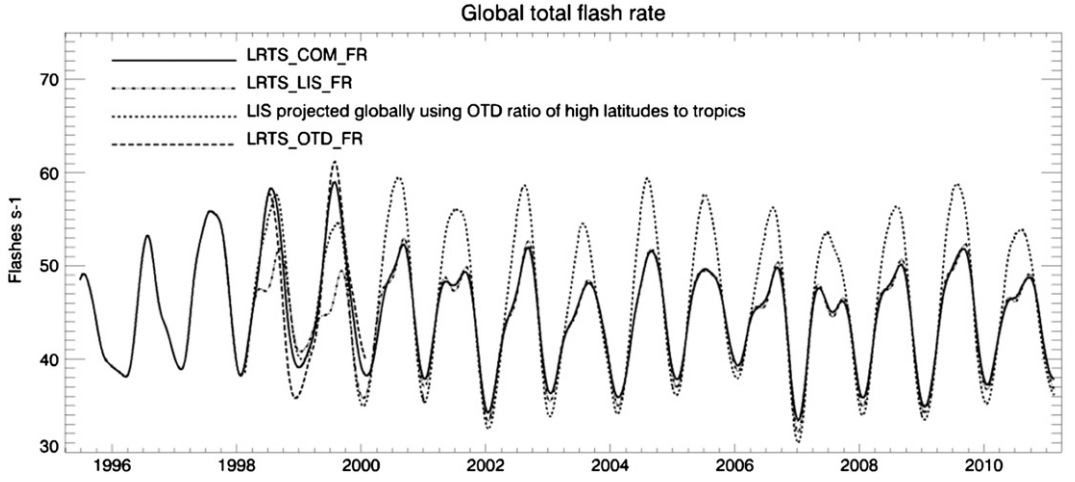

Fig. 4. Global flash rate (flashes s^{-1}) time series computed from LRTS. See text for details.

Please cite this article as: Cecil, D.J., et al., Gridded lightning climatology from TRMM-LIS and OTD: Dataset description, Atmos. Res. (2012), doi:10.1016/j.atmosres.2012.06.028

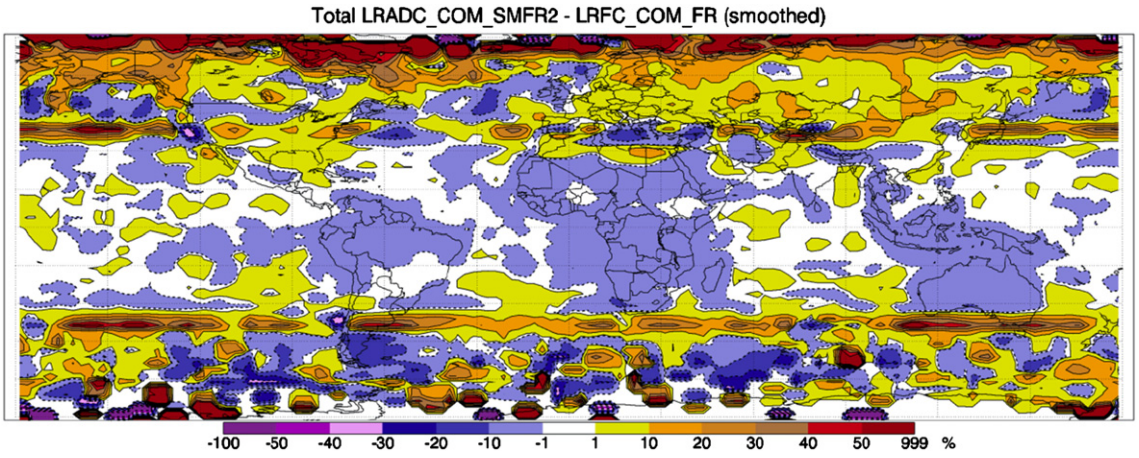

Fig. 5. Percentage difference between mean annual flash rate taken from LRADC (equally weighting each day of year and time of day) and from LRFC. 7.5°×7.5° boxcar smoothing has been applied here to LRFC, in order to match that in LRADC.

hence the confidence in the estimates) is worse. Even there, the agreement is usually within 30% and sometimes much better than that. Note that the LRFC grid must be smoothed to match LRADC for this comparison, otherwise there are large differences in places with sharp gradients of flash rate (e.g., along coasts).

The peak annual flash rate at 0.5° scale in HRFC (Fig. 2a) is 160 fl km^{-2} yr^{-1} in eastern Congo. A broad region of central Africa exceeds 30 fl km^{-2} yr^{-1}. Most land regions in the tropics and subtropics—except for arid regions—exceed 10 fl km^{-2} yr^{-1}. For more details on local extrema using a higher resolution grid, including a maximum associated with Lake Maracaibo (Venezuela) that exceeds the eastern Congo values, see Albrecht et al. (2011). The global average from this dataset is 46.1 fl s^{-1} (very similar to that reported by Christian et al., 2003 from the OTD climatology by itself), 2.9 fl km^{-2} yr^{-1}, 1.46 billion flashes yr^{-1}. About 90% of that comes from within the LIS domain (+/−38°). Without merging the LIS and OTD data, the 1998–2010 LIS climatology has 2% more flashes in the +/−38° domain than does the 1995–2000 OTD. Accounting for both the annual cycle and diurnal cycle with LRADC as in Fig. 5, the global mean flash rate comes to 46.0 fl s^{-1}. Computing it from any of the LIS–OTD combined products, the mean flash rate only ranges from 45.4 fl s^{-1} (from the mean of the diurnal cycle, LRDC) to 46.5 fl s^{-1} (from the mean of the annual cycle, HRAC). As pointed out by Christian et al. (2003), these values are less than half the 100 fl s^{-1} estimate proposed by Brooks (1925), and also less than the estimates from Orville and Spencer (1979) (123 fl s^{-1} from Defense Meteorological Satellite Program observations at dusk, and 96 fl s^{-1} from observations at midnight) and from Mackerras et al. (1998) (65 fl s^{-1}

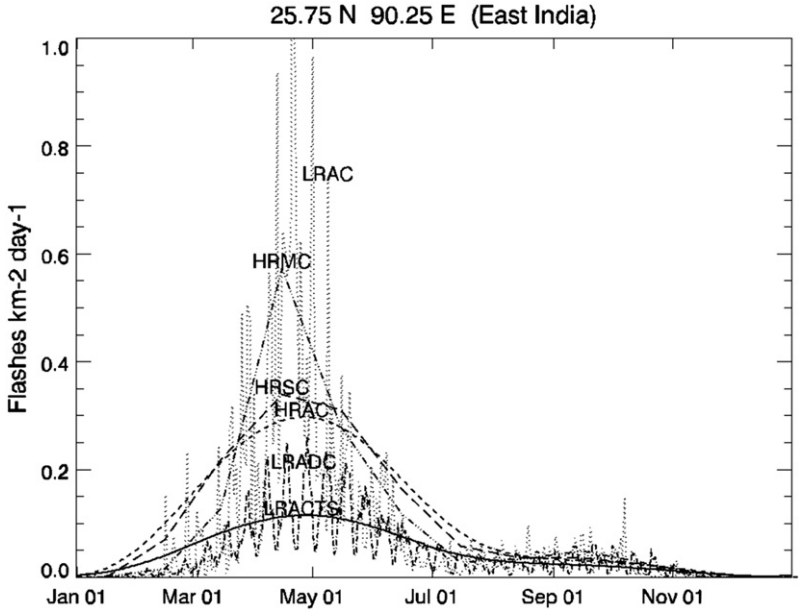

Fig. 6. Annual cycle of flash rate (fl km^{-2} day^{-1}) for grid box in East India. To reduce clutter, the annual cycle from LRADC is only plotted every tenth day.

Please cite this article as: Cecil, D.J., et al., Gridded lightning climatology from TRMM-LIS and OTD: Dataset description, Atmos. Res. (2012), doi:10.1016/j.atmosres.2012.06.028

estimated from a combination of observations and models). The global measurements from LIS and OTD give the first estimates that justify a precision down to a few flashes per second, as opposed to just getting the correct order of magnitude.

3.2. Annual cycle of lightning

Several of these products specify the annual cycle of lightning flash rates. The animation of HRAC is the most aesthetically pleasing, but otherwise there is not much reason to bother with a grid with 365 daily values that have been subjected to 111-day smoothing. Similar information content can be found from the smaller HRSC, with 12 monthly grids that have been subjected to 91-day smoothing. If less smoothing is desired, HRMC has the 12 monthly grids subjected to 31-day smoothing, and LRAC allows the user to choose his or her own smoothing for the 365 daily grids.

Fig. 6 compares the annual cycle of flash rate from the different products, for a grid box in the Brahmaputra Valley of East India having the highest HRMC monthly mean flash rate (17 fl $km^{-2}mo^{-1}$) anywhere. The LRAC curve is much too noisy to take literally. The monthly resolution of HRMC captures the sharp April peak of lightning in this area. Lightning subsequently decreases in this region during the monsoon season that usually begins in early June, but increases further north and west. The August averages for grid boxes in northern Pakistan also exceed any monthly averages from Africa, despite central Africa having the greatest yearly average. The longer smoothing windows for HRSC and HRAC dampen the amplitude of the pre-monsoon peak in Fig. 6, and extend high flash rate values into the monsoon season when the true flash rates are low. LRACTS shows the smoothest curve with the lowest amplitude, because it uses a large time window for smoothing, plus it smooths over a 7.5°×7.5° grid box. LRADC also smooths over this larger grid box, but shows the diurnal range of flash rates. For this grid box, the flash rates peak between 16 and 18 UTC (22–00 local), with values a factor of five greater than during the early morning minimum between 02 and 04 UTC (08–10 local).

Fig. 7 multiplies the flash rates in HRMC and LRAC by the corresponding grid box sizes, and sums all grid boxes to estimate the annual cycle of global flash rate. Again the need to smooth the LRAC product is obvious, and any real variability appears to be adequately represented by the monthly HRMC. The OTD–LIS combined HRMC product estimates a minimum global flash rate of 35 flashes s^{-1} in February, and a maximum 60 flashes s^{-1} in August. From October through April, the estimate from LIS is within a few percent of the combined estimate, despite LIS not observing high latitudes. Other than during boreal summer, the LIS domain does include most of the global lightning. This LIS estimate is probably a bit too high, because the high flash rates near the edge of the LIS domain in northern Argentina and southern Africa get smoothed into un-sampled locations that should actually have very low flash rates.

3.3. Diurnal cycle of lightning

For analysis of the diurnal cycle, the LRDC product is probably appropriate for most purposes, although additional spatial smoothing of the 2.5° grid is recommended. Fig. 8a compares the LRDC flash rate diurnal cycles from LIS, OTD, and the combined product for the same grid box in East India as that shown previously. All three show a local maximum in flash rate in early afternoon (between 12 and 15 local time), but OTD mostly misses the strong overnight lightning maximum recorded by LIS. At 30° latitude, LIS has a large sample size and contributes heavily to the combined product. This example demonstrates that the diurnal cycle derived from OTD alone (whether in the OTD product, or the

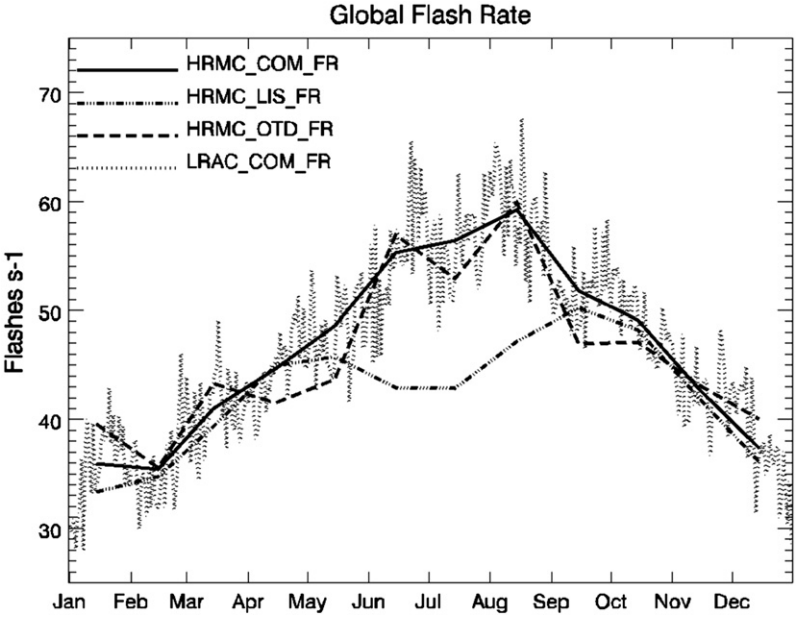

Fig. 7. Annual cycle of global flash rate, computed from HRMC and from LRAC.

Please cite this article as: Cecil, D.J., et al., Gridded lightning climatology from TRMM-LIS and OTD: Dataset description, Atmos. Res. (2012), doi:10.1016/j.atmosres.2012.06.028

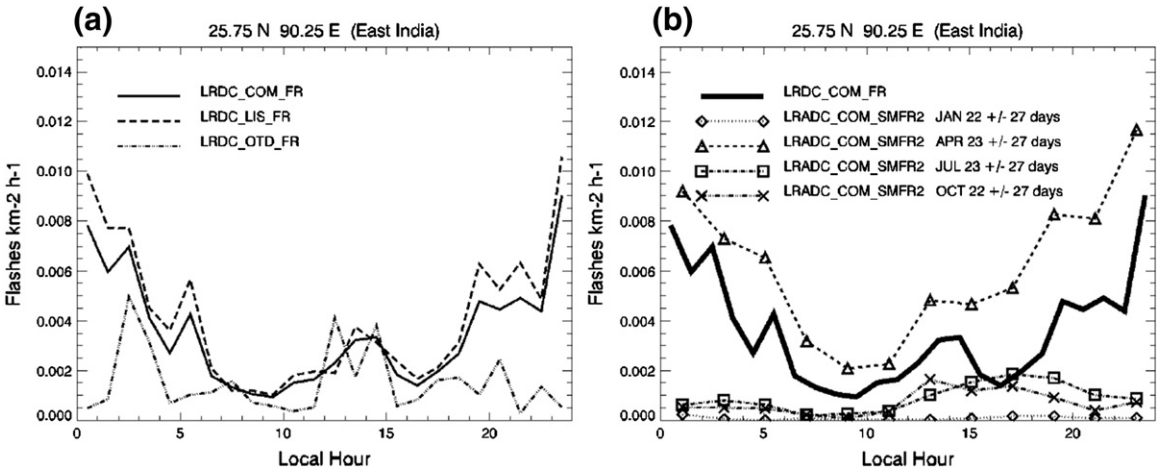

Fig. 8. Diurnal cycle of flash rate (fl km^{-2} h^{-1}) for grid box in East India. (a) LRDC diurnal cycle from LIS, OTD, and combined product. (b) LRADC diurnal cycle from Jan–Feb, Apr–May, Jul–Aug, and Oct–Nov, compared to mean diurnal cycle from LRDC_COM_FR. LRADC diurnal cycle converted here to local time for this grid box (UTC + 6 h).

combined product at high latitudes) should be treated with extra caution. Even with the relatively large sample from LIS, one should use caution when interpreting details from a particular 2.5° grid box. Most adjacent grid boxes do not show the late afternoon flash rate minimum seen in Fig. 8a, or as strong an overnight maximum as in Fig. 8a.

For some locations or some study topics, it is more appropriate to consult the LRADC product for the diurnal cycle at a particular time of year. Blakeslee et al. (this issue) examine seasonal variations in the diurnal cycle and its implications for the global electric circuit. Fig. 8b shows seasonal variations of the diurnal cycle for the same grid box in East India. The time of day has been converted from UTC in LRADC to local time for this grid box at 90° E. The peak flash rate from LRADC for this grid box comes from 23 April (+/−27 days smoothing), between 16 and 18 UTC (22–24 local). Diurnal flash rate curves for this day and for three other times of year are plotted in Fig. 8b. The maximum near local midnight is only seen during the high flash rate pre-monsoon season (April–May). During other seasons, there is a much lower amplitude late afternoon maximum, peaking between 10 and 12 UTC (16–18 local). Although LRADC is presented on a 2.5° grid, it uses 7.5° smoothing. That smoothing removes the late afternoon local minimum that was noted from LRDC, and is very likely not a robust feature of the diurnal cycle here.

3.4. Multi-year time series

The largest (and most unwieldy) of these gridded LIS–OTD datasets is the LRTS time series. As with HRAC, the smoothed daily values from LRTS can contribute to an aesthetically pleasing animation, but the monthly values from LRMTS probably contain all the scientifically robust information in a more practical, smaller dataset. For example, Hernandez and Schumacher (2008) used the LRMTS to examine the quasi-biennial oscillation. Fig. 9 compares the time series from the different products, for that same grid box in East India. The small differences between the combined flash rate and the LIS flash rate after OTD stopped

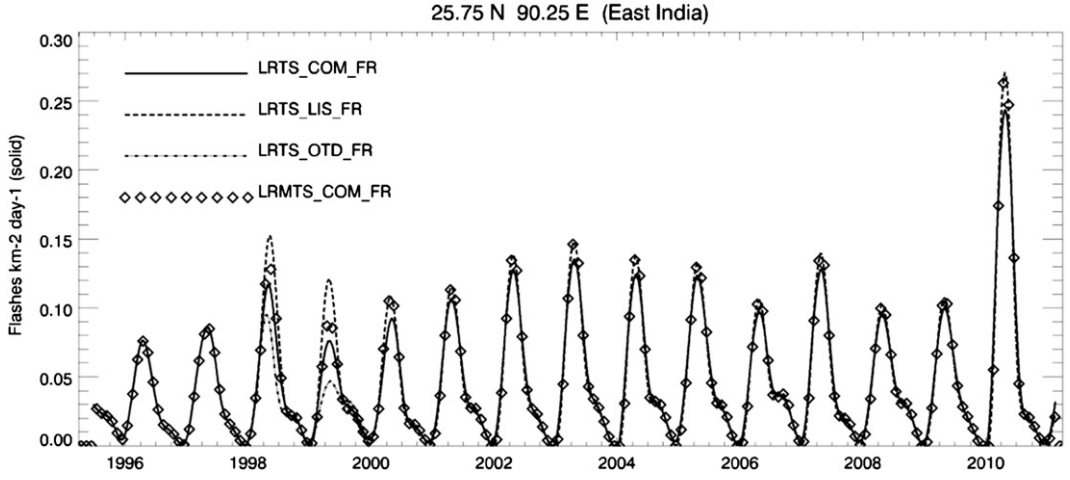

Fig. 9. LRTS and LRMTS flash rate time series for the same grid box as in Fig. 7.

Please cite this article as: Cecil, D.J., et al., Gridded lightning climatology from TRMM-LIS and OTD: Dataset description, Atmos. Res. (2012), doi:10.1016/j.atmosres.2012.06.028

collecting data in 2000 are due to different smoothing windows. The combined product always uses a 111-day smoothing, but LIS uses a 99-day smoothing. The monthly LRMTS combined flash rate differs from the LRTS combined flash rate, because it weights the LIS observations more heavily than the OTD observations when there is overlap. This is appropriate, since LIS is a higher quality instrument on a more stable platform. The LRMTS combined flash rate also matches the LRTS LIS flash rates (99-day smoothing) after OTD data collection stopped. Although we make the daily LRTS grids available, the monthly LRMTS grids are recommended for almost all scientific purposes.

4. Summary

Gridded climatologies of lightning flash rate have been derived from the OTD (1995–2000) and LIS (1998–ongoing) satellite sensors. Several different products are now available to the public, as listed in Table 1 and thoroughly described in Section 2. These include 0.5°×0.5° and/or 2.5°×2.5° grids of total annual flash rate, annual cycle of flash rate, diurnal cycle of flash rate, and annual cycle of the diurnal cycle using data from mid-1995 through 2010. Daily and monthly time series of flash rate on a 2.5°×2.5° grid with 7.5° spatial smoothing and ~3 month temporal smoothing have also been produced, spanning from mid-1995 to early 2011. Some examples of the data products and how they can be used are given in Section 3. Recommendations for choosing which data products to use are summarized below. For all products, extra caution is warranted at high latitudes were the sample size is small (having come from OTD only).

For simple estimates of total annual flash rate, HRFC and LRFC are straightforward to use. Their flash rate estimates agree to within a few percent with estimates that account for uneven sampling of the annual cycle and diurnal cycle. For estimates of the annual cycle, the monthly climatology HRMC is probably suitable for most users. The daily climatology HRAC has so much temporal smoothing, and it is really suited for aesthetically pleasing animations more than for scientific analysis. The daily climatology LRAC, on the other hand, has no temporal smoothing. Some smoothing is certainly necessary due to the nature of the sampling, but with LRAC the user can determine what type of smoothing to apply.

The diurnal cycle is estimated on a 2.5° grid in LRDC, and the diurnal cycle as it varies through the year is estimated in LRADC. LRADC is smoothed with a 7.5° filter. For places with distinct seasonality, LRADC may be more appropriate to use. For places where much of the total annual lightning occurs in a particular season, the LRDC diurnal cycle should be similar to the LRADC diurnal cycle for that season. Users are especially encouraged to be aware of the smoothing noted in Table 1 for LRADC, and to be aware of the potential need for more smoothing with any of the products. The diurnal cycle plotted from LRDC in Fig. 8a would look dramatically different using one 2.5° grid box to the north or west, for example, and the sample size for each individual grid box is not robust enough for accurate hourly estimates.

For time series analysis, the monthly LRMTS product is strongly recommended. The daily product LRTS has over 3 months worth of smoothing for each daily grid, so one might as well use the more manageable LRMTS. LRMTS also has a better combination of the LIS and OTD flash rates, giving more weight to the higher quality LIS data. As with all products, the time series values for data points where LIS was unavailable (i.e., high latitudes or time before 1998) should be treated with extra caution.

Supplementary related to this article can be found online at http://dx.doi.org/10.1016/j.atmosres.2012.06.028.

Acknowledgments

This research benefits from over two decades of work by past and present members of the lightning team associated with NASA MSFC. In particular, the gridded climatologies were updated using source code developed by Dennis Boccippio. Sponsorship and support for the OTD and LIS data is from the NASA Earth Observing System and the Tropical Rainfall Measuring Mission. LIS and OTD data, including the gridded climatologies produced here, are distributed by the NASA EOSDIS Global Hydrology Resource Center DAAC, Huntsville, AL, USA, http://thunder.nsstc.nasa.gov.

References

Adler, R.F., Wang, J.-J., Gu, G., Huffman, G.J., 2009. A ten-year tropical rainfall climatology based on a composite of TRMM products. J. Meteor. Soc. Jpn. 87A, 281–293.

Albrecht, R., et al., 2011. The 13 years of TRMM Lightning Imaging Sensor: from individual flash characteristics to decadal tendencies. *XIV Int. Conf. Atmos. Elec.*, Rio de Janeiro, Brazil.

Blakeslee, R.J., Mach, D.M., Bateman, M.G., Bailey, J.C., this issue. Seasonal variations in the lightning diurnal cycle and implications for the global electric circuit. *Atmos. Res.*

Boccippio, D.J., Koshak, W.J., Blakeslee, R.J., 2002. Performance assessment of the Optical Transient Detector and Lightning Imaging Sensor, I, predicted diurnal variability. J. Atmos. Oceanic Technol. 19, 1318–1332.

Brooks, C.E.P., 1925. The distribution of thunderstorms over the globe. Geophys. Memo. 3 (24), 147–164.

Bürgesser, R.E., Nicora, M.G., Ávila, E.E., 2012. Characterization of the lightning activity of "Relámpago del Catatumbo". J. Atmos. Sol. Terr. Phys., http://dx.doi.org/10.1016/j.jastp.2012.01.013

Cecil, D.J., Blankenship, C.B., 2012. Toward a global climatology of severe hailstorms as estimated by satellite passive microwave imagers. J. Clim. 25, 687–703.

Christian, H.J., et al., 2003. Global frequency and distribution of lightning as observed from space by the Optical Transient Detector. J. Geophys. Res. 108 (D1), 4005, http://dx.doi.org/10.1029/2002JD002347.

Hernandez, C.A., Schumacher, C., 2008. The QBO's influence on lightning production in the tropics. *28th Conf. On Hurricanes and Trop. Meteor.*, Amer. Meteor. Soc., Orlando, FL.

Kummerow, C., et al., 2000. The status of the Tropical Rainfall Measuring Mission after 2 years in orbit. J. Appl. Meteorol. 39, 1965–1982.

Mackerras, D., Darveniza, M., Orville, R.E., Williams, E.R., Goodman, S.J., 1998. Global lightning: total, cloud and ground flash estimates. J. Geophys. Res. 103 (D16), 19,791–19,809, http://dx.doi.org/10.1029/98JD01461.

Orville, R.E., Spencer, D.W., 1979. Global lightning flash frequency. Mon. Weather Rev. 107, 934–943.